Polish J. Chem., **78**, 389–408 (2004)

X-ray, $^{1}H/^{13}C$ 2D and 3D NMR Studies of the Structures of Davallene and Adipedatol, Two Triterpenes Isolated from American *Adiantum capillus-veneris*

by C.K. Jankowski*[1], A. Aumelas[1], P. Thuéry[2], R. Reyes-Chilpa[3], M. Jimenez-Estrada[3], H. Barrios[3] and E. Diaz[3]

[1]*Département de Chimie et Biochimie, Université de Moncton, Moncton, Nouveau-Brunswick, Canada, E1A 3E9*
[2]*CEA/Saclay, DSM/DRECAM/SCM (URA 331), Bât. 125, 91191 Gif-sur-Yvette, France*
[3]*Instituto de Quimica, Universidad Nacional Autonoma de Mexico, Circuito Exterior, Ciudad Universitaria, Coyoacan 04510 Mexico D.F., Mexico*

(Received November 25th, 2003)

Two triterpenic compounds, Davallene **1** and Adipedatol **2** were isolated from the roots of Mexican *Adiantum capillus-veneris* L. (*Adiantaceae*). The structures of both compounds are discussed on the basis of new 2D and 3D NMR spectroscopic and single crystal X-ray diffraction data.

Key words: triterpenes from *Adiantum*, NMR 1D and 2D of triterpenes, X-rays – 2D, 3D NMR of triterpenes

Adiantum capillus-veneris is one of the most widely-distributed fern species in the world. It can be found in Asia, Africa, Europe and the Americas [1]. Previous phytochemical studies of *A. capillus-veneris* have reported the presence of a number of hopane and oleane triterpenoids [2,3]. Differences in chemical composition have been found in samples from Asia and Africa [4,5], but less is known about the specimens from the Americas. *A. capillus-veneris* is also widely spread in Mexico, where it is commonly used in traditional folk medicine. Infusions of the fern are used in many applications for a variety of ailments, such as against cough, after childbirth, as a remedy for excessive menstrual flux and as a soft abortifacient. The infusion is also administered for minor liver and spleen disorders [6].

To our knowledge this is the first time that Davallene **1** and Adipedatol **2** (Scheme 1) have been isolated from Mesoamerican *A. capillus-veneris*. Davallene is widely found in ferns [3], while Adipedatol has previously been obtained only from Japanese *Adiantum pedatum* [4]. Its structure was determined spectroscopically and through chemical transformations [5], with the exception of the stereochemistry of C-20. Although structures of both triterpenes were proposed several years ago [4,7], the reported features of their NMR spectra have offered only limited structural information, since their proton-NMR spectra were recorded at <300 MHz frequencies.

* Author to whom correspondence may be addressed. Email: jankowc@umoncton.ca

Scheme 1

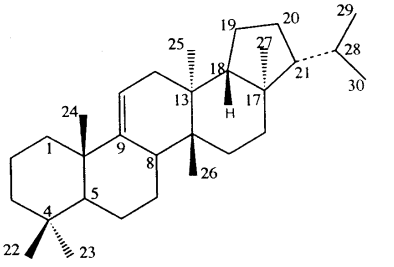

Davallene **1**

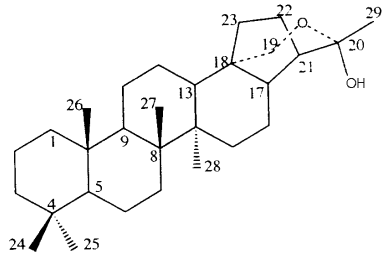

Adipedatol **2**

Consequently, the proton resonances of these relatively simple molecules neither having more than a single functional group (one oxygenated, the other with a double bond) are highly overlapped and the specific assignment of several chemical shifts of the triterpene structures remains, at best, speculative.

In the present work, first of all, the mass spectra of the two triterpenes were recorded in Electron Impact, Chemical Ionisation, Fast Atom Bombardment and Electrospray Ionisation modes together with the high-resolution determination of the exact mass of some peaks in the area near the molecular ion masses. Both triterpenes, however, display somehow confusing similarities in their mass spectra. The mass spectra of **1** and **2** as recorded in FAB PI mode show an intense peak at m/z 411 which was mistakenly thought to represent $(M+H)^+$ ion whereas in only one case was this in fact correct. For **1**, the exact mass measured for the protonated molecular ion was at 410.3913 showing the hydrocarbon structure, whereas for **2** the mass at 411.3627 displayed rather an oxygen-containing fragment. The second, smaller, peak in FAB for **2** was however measured to have the exact mass corresponding to $C_{29}H_{47}O_2$ and could be assigned to the $(M+H)^+$ peak for this compound (with m/z 427.3576). In the spectrum of **1** the M+H peak is also accompanied by the intense (M–1) ion. The ammonia-PI-chemical ionisation mass spectra of both terpenes showed the $(M+H)^+$ ions at their correct masses, with the important $(NH_4)^+$ adduct ion for the oxygenated **2**. In these cases, while neither EI, CI or FAB mass spectra cannot provide us with a clear choice among the closely-related isomeric structures, single crystal X-rays diffraction enable us to advance the issue (assuming the availability of crystals of the requisite size and quality).

The identification of the triterpenic structures by high resolution, multinuclear and polydimensional NMR is based, in this study, on 2D H/H correlation spectra, such as COSY [8–10] and TOCSY [11], as well as on H/C heteronuclear correlation, in particular HSQC [12] and HMBC [13] experiments. Following these series of experiments, a correct assignment of proton and carbon signals is proposed for the entire triterpene. The specific linkages of segments of the molecule skeleton parts were first tested using homo- and hetero-correlated COSY experiments, in order to establish the proton-proton connectivity pattern. In both triterpenes, however, the partial proton sequences are terminated by quaternary carbons, which significantly impeed this approach. This difficulty can sometimes be overcome by using HMBC experiments, which would provide information about protons coupled to quaternary carbons through the proton-carbon 2δ and 3δ bonds and newer, recently-emerged 3D NMR techniques [14] in particular, DEPT-HSQS and HSQC-TOCSY [15–17].

In this paper, we report on the use of 2D and 3D NMR experiments to unambiguously interpret and completely assign both the proton and carbon spectra, as well as the stereochemical features of the triterpenes **1** and **2**. As it is often the case in terpene chemistry, additional information (such as molecular formulae deduced from the mass spectroscopy) enabled to confirm the formulas $C_{30}H_{50}$ for Davallene (**1**) and $C_{29}H_{48}O_2$ for Adipedatol (**2**). The single-crystal X-ray diffraction results were then used as a constant lead for the design and interpretation of NMR experiments.

RESULTS AND DISCUSSION

In the following two sections the structural features of both triterpenes are discussed separately with extensive reference to their NMR polydimensional spectra.

Davallene (1): The general appearance of the NMR proton spectrum of **1** displays, first, six methyl singlets at δ 0.74 ,0.76, 0.82, 0.86, 0.88 and 1.05 ppm, respectively. Two doublets in the same area at 0.89 and 0.83 (J = 7.0 Hz) are assigned to coincidentally isochronous methyls of an isopropyl group. One broad doublet is found at δ 2.05 (1H), and a second at δ 1.85 (1H), these together with the multiplet at δ 1.78 (1H), the broad triplet at δ 0.95 and the highly overlapped multiplets at 1.05 through 1.70 complete the spectrum. The integration of signals in this compound accounts well for all fifty protons from the 1D proton NMR spectrum.

In the ^{13}C spectrum of **1** (noise-decoupled) we observed twenty eight signals, one carbon signal accounted for two nuclei, six quaternary carbons (one olefinic at 151.7 and five aliphatic at 30.0, 38.0, 33.6, 37.6 and 43.0), ten methylenes at δ 41.5, 19.6 (two carbons), 42.4, 20.1, 36.1, 29.3, 36.8, 17.9 and 28.2 followed by six methins signals at 115.6 (olefinic) and 44.9, 40.0, 52.0, 59.2 and 30.8.

Data from the proton-proton COSY experiments, as well as from TOCSY, were transformed from the contour plot and are listed in Table 1. Both series of experiments confirmed the connectivity of the vicinal protons. Conversely, heteronuclear experiments HSQC and HMBC, as summarized in Table 1, provided interesting complementary images of the couplings, as deduced from the cross peaks ($^{1}J_{CH}$) and from

the long range $^{2}J_{CH}$ and $^{3}J_{CH}$ couplings displayed from the latter two experiments (Figs. 1–3). As a result of these experiments, all protonated carbons were separated into segments separated by quaternary carbons. However, even after these heteronuclear analysis, several different isomeric structures remain as possible explanations for these schemes of coupling. In order to proceed to an unambiguous identification of spectra the NMR spectra were systematically analysed beginning with the well--identified isopropyl group.

Table 1. Davallene* **1**.

Posit.	DEPT	δ H1^{+}	δ C^{+}	TOCSY$^{\Delta}$	HMBC†	HSQC TOCSY$^{\#}$
1	CH_2	1.88, 1.12	41.5	1.55^{2}, 1.40^{2}, 1.30^{3} 1.10^{3}, 1.88^{1}	1.05^{24} 1.12^{1}	1.88^{1}, 1.12^{1}, 1.55^{2},1.40^{2} 1.35^{3}, 1.10^{3}
2	CH_2	1.40, 1.55	19.6			1.88^{1}, 1.55^{2}, 1.40^{2}, 1.10^{3}, 1.40^{2}, 1.35^{3}, 1.10^{3}
3	CH_2	1.35, 1.10	42.4	1.35^{3}, 1.55^{2}	0.86^{22}, 0.88^{23}, 1.10^{3}	1.88^{1}, 1.12^{1}, 1.52^{2}, 1.40^{2}, 1.35^{3}, 1.10^{3}
4	C		33.6		0.82^{22}, 0.88^{23}	
5	CH	1.25	44.9	2.05^{8}, 1.70^{6}, 1.52^{6}	1.25^{5}, 0.88^{23}, 0.86^{22}	1.70^{6}, 1.60^{7}, 1.52^{6}, 1.32^{7}, 1.25^{5}, 2.05^{8}
6	CH_2	1.70, 1.52	19.6	2.05^{8}, 1.58^{7}, 1.56^{2} 1.30^{7}, 1.25^{5}	1.70^{6}, 1.52^{6}, 1.58^{7}	2.05^{8}, 1.70^{6}, 1.58^{7}, 1.25^{5}
7	CH_2	1.58, 1.30	17.9		1.52^{6}	2.05^{8}, 1.70^{6}, 1.58^{7}, 1.30^{7}, 1.52^{6}
8	CH	2.05	40.0	1.70^{6}, 1.58^{7}, 1.52^{6} 1.30^{7}	0.74^{26}	2.05^{8}, 1.70^{6}, 1.52^{6}, 1.58^{7}, 1.30^{7}
9	C		151.7		1.05^{24}, 5.3^{11}	
10	C		38.0		1.05^{25}	
11	CH	5.30	115.6			
12	CH_2	1.60, 1.52	36.8			2.05^{8}, 1.50^{12}, 1.60^{12}, 0.82^{25}
13	C		36.8			
14	C		37.6		0.82^{25}, 0.74^{26}, 1.60^{12}, 1.52^{12}	
15	CH_2	1.40, 1.30	29.3	1.40^{15}, 0.74^{26}, 1.30^{15}	0.74^{26}	1.40^{15}, 1.30^{15}, 1.64^{16}
16	CH_2	1.64, 1.40	36.1	1.40^{15}, 1.30^{15}, 0.76^{27}		1.65^{16}, 1.40^{15}, 1.30^{15}, 0.76^{27}
17	C		43.0		0.76^{27}, 1.32^{19}	
18	CH	1.53	52.0		0.76^{27}, 0.82^{25}	1.30^{19}, 0.95^{21}, 0.83^{29}, 0.89^{30}, 1.80^{20}, 1.53^{18}, 1.32^{19}, 1.20^{20}
19	CH_2	1.30, 1.32	20.1		1.30^{19}, 1.20^{20}	
20	CH_2	1.82, 1.20	28.2	1.20^{20}, 1.53^{18}, 1.45^{28} 1.30^{19}, 1.32^{19}		1.32^{19}, 1.30^{19}, 1.20^{20}, 0.83^{29}, 1.82^{20}, 1.53^{18}, 0.95^{21}, 0.89^{30}

Table 1. (continuation)

21	CH	0.95	59.2		0.83^{29}, 0.89^{30}, 0.76^{27}	1.82^{20}, 1.53^{18}, 1.45^{28}, 0.89^{30}, 1.32^{19}, 1.25^{20}, 0.95^{21}, 0.83^{29}
22	CH_3	0.86	32.8		0.88^{23}	0.86^{22}, 0.88^{23}
23	CH_3	0.88	21.7		0.86^{22}	0.88^{23}, 086^{22}
24	CH_3	1.05	25.0			1.05^{24}
25	CH_3	0.82	15.9			
26	CH_3	0.74	15.4			
27	CH_3	0.76	14.0		1.52^{18}	
28	CH	1.45	30.8	0.89^{30}, 0.83^{29}, 1.82^{20}	0.95^{21}, 1.53^{18}, 1.30^{19}, 1.32^{19}	1.45^{28}, 0.89^{30}, 0.83^{29}
29	CH_3	0.83	23.0	0.95^{21}, 1.25^{20}, 1.32^{19} 1.45^{28}, 1.53^{18}, 1.30^{19}, 1.32^{19}, 1.82^{20}		0.83^{29}, 0.89^{30}, 0.95^{21}, 1.45^{28}
30	CH_3	0.89	22.1	0.95^{21}, 1.25^{20}, 1.32^{19}, 1.45^{28}, 1.53^{18}, 1.82^{20}		0.89^{30}, 0.83^{29}, 0.95^{21}, 1.45^{28}

*Recorded in $CDCl_3$ 600/150 MHz ($^{1}H/^{13}C$); $^{+}$ assignments confirmed by HSQC experiments; † indicate $^{2}J_{CH}$, $^{3}J_{CH}$, C position with neighbouring protons. Superscript beside proton chemical shifts indicate which proton is involved in the C/H interaction; $^{\Delta}$ Indicate ^{1}H-^{1}H interaction; $^{\#}$ Indicate C position with neighbouring protons.

Both methyls at $\delta = 0.83$ and 0.89 were correlated to the methine at 1.45 and to the broad triplet at $\delta = 0.95$. This latter methine proton was correlated to the methylenes at 1.80 and 1.20 and with protons at 1.30 and 1.32. These connectivities match well with the fragment C_{18}–C_{19}–C_{20}–C_{21}–C_{28}–C_{29}–C_{30}, separated by C_{13} and C_{17}, corresponding to the five member ring moiety (ring E) of **1**.

The methine proton (C-8) at $\delta = 2.05$ (broad doublet) correlates well with the cross-peak at $\delta = 1.30$ and 1.58 (C-7 methylene) and with the olefinic proton al $\delta = 5.30$ (quintet, J = 2.3, 5.2, 2.3 Hz *via* vicinal and allylic couplings, respectively). The olefinic proton (H-11) correlates with methylene protons at $\delta = 1.52$ and 1.60 (C-12). From the diagonal peak of one of the C-7 methylene protons, we were able to find first the methylene proton cross peaks at $\delta = 1.52$ and 1.70, and then the correlation of H-6 and H-6' with the methine (C-5) at $\delta = 1.25$. These correlations enabled us to establish the proton assignment of rings B and C. Because the remaining chemical shift protons on C_1–C_2–C_3 (ring A) and C_{15}–C_{16} (ring D) display high overlapped signals from δ 1.70 to 1.00, we decided to use the HSQC $^{1}H/^{13}C$ ($^{1}J_{CH}$) correlation spectrum, in order to find the particular proton chemical shifts of this segment. In this way, it was possible to observe the methylene protons on the aforementioned A- and D-rings, C-1, C-2, C-3, as well as those of C-15 and C-16 and finally the methine proton (C-18) (Fig. 1). Fig. 3 displays a 3D $^{1}H/^{13}C$ NMR correlation spectrum (HSQC-TOCSY) so as to show how we identified C-2's methylene protons (C-2 $\delta_C = 19.6$, $\delta_H = 1.55$, 1.40).

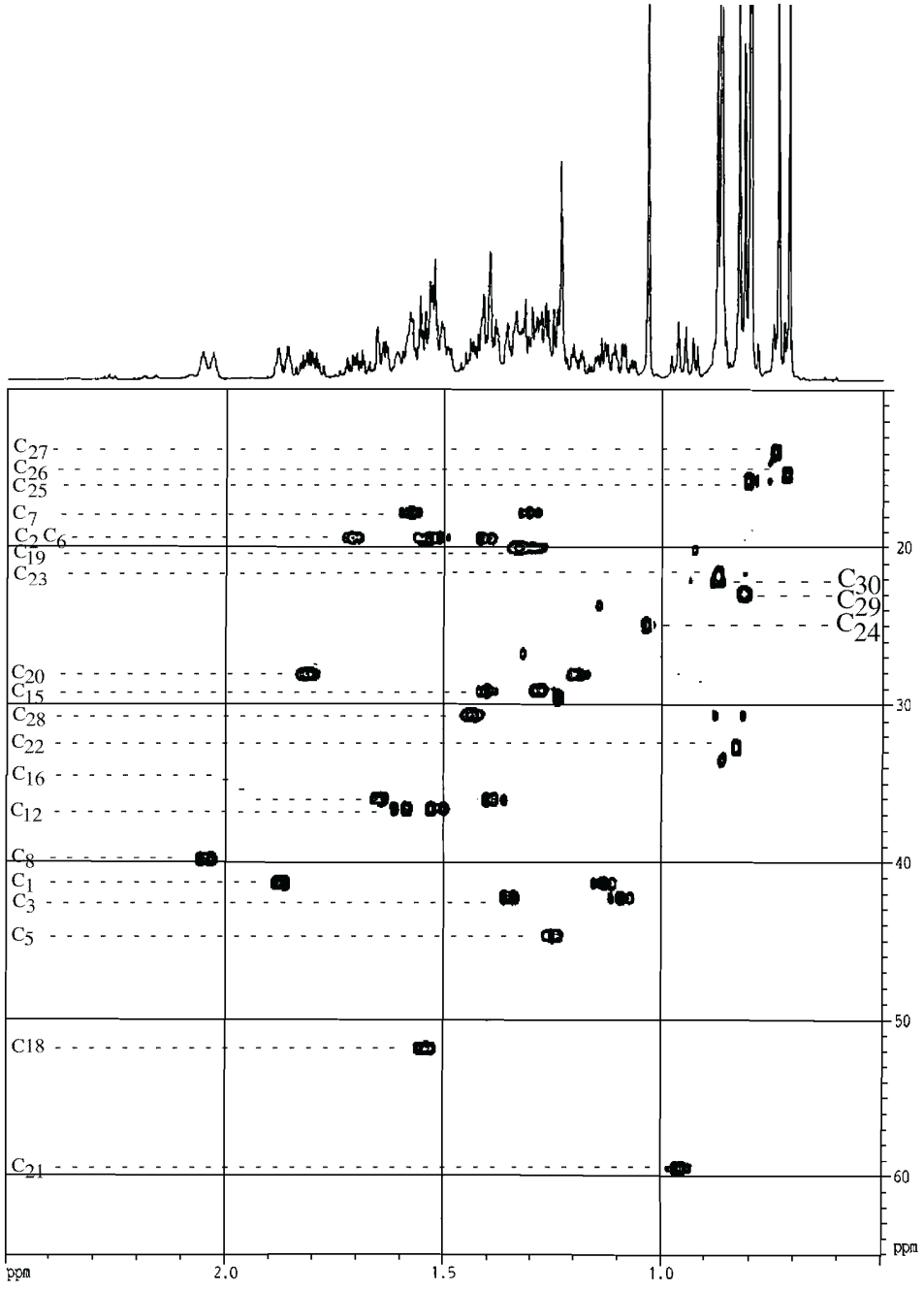

Figure 1. HSQC spectrum of Davallene **1** recorded in $CDCl_3$ solution at $^{1}H/^{13}C$ 600/150 MHz.

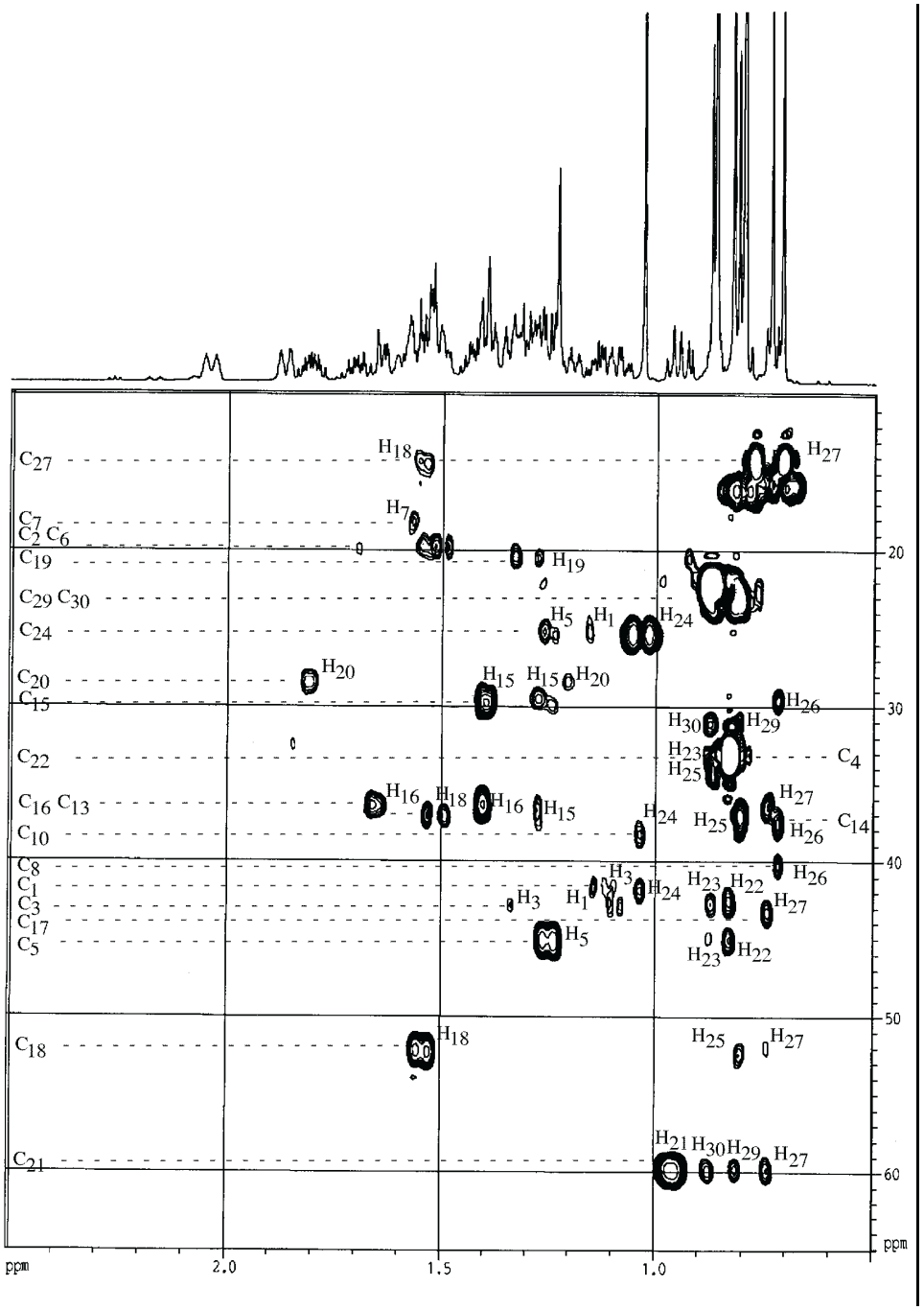

Figure 2. HMBC spectrum of Davallene **1** recorded in $CDCl_3$ solution at $^{1}H/^{13}C$ 600/150 MHz.

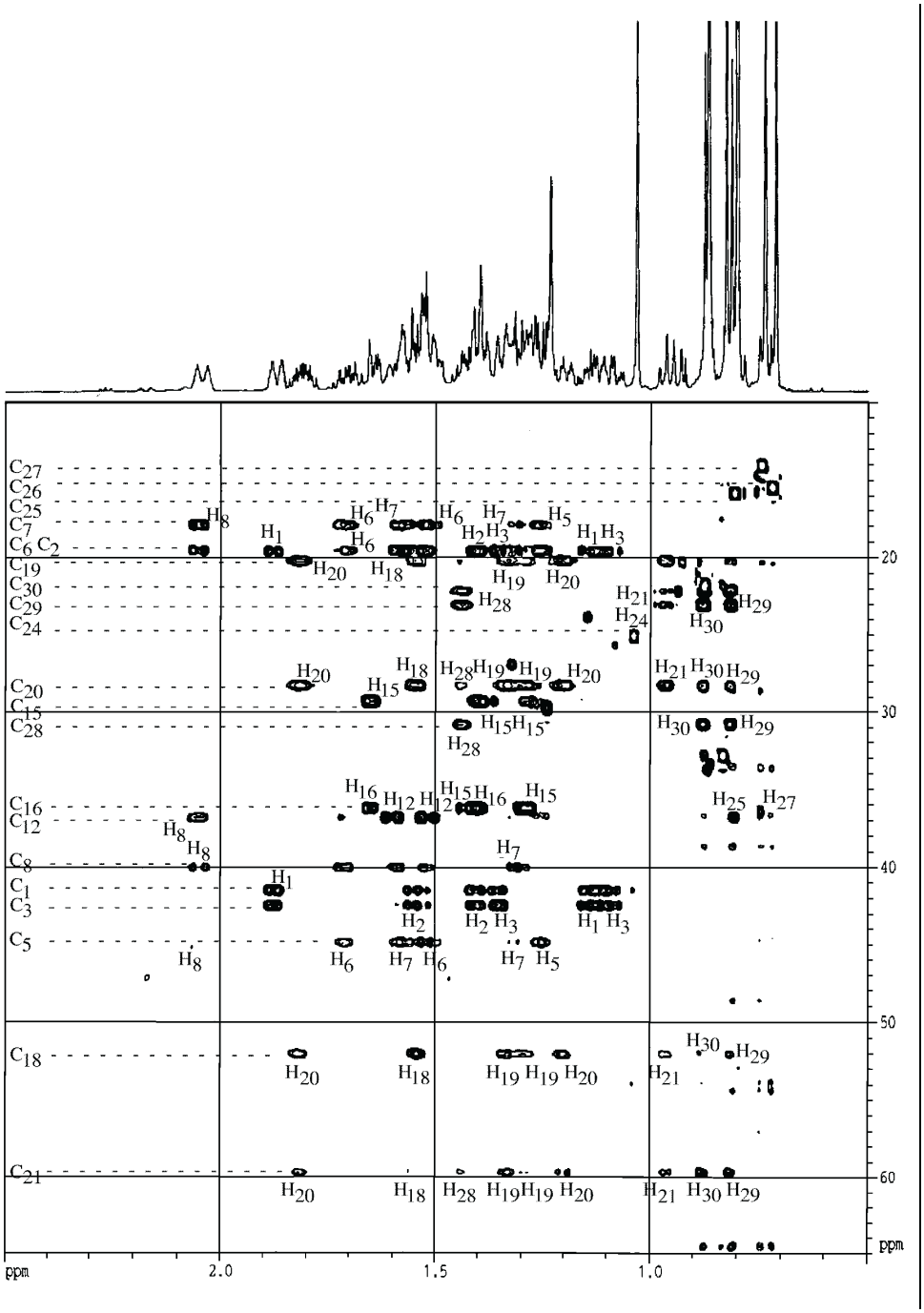

Figure 3. HSQC-TOCSY spectrum of Davallene **1** recorded in $CDCl_3$ solution at $^{1}H/^{13}C$ 600/150 MHz.

Since this fragment is framed by the quaternary carbons C-4 and C-10, the HSQC-TOCSY spectrum displayed in Fig. 3 shows all corresponding correlations, and consequently improves the interpretation. Similarly, the C_{15}–C_{16} segment of the molecule (limited by the quaternary carbons C-14 and C-17) clearly shows the $^{1}H/^{13}C$ correlations on C-15 $\delta_C = 29.3$; C-16 $\delta_C = 36.1$ in its HSQC-TOCSY spectrum *via* well identified cross peaks at $\delta = 1.40$, 1.30 (H-15, H-15') as well as at $\delta = 1.64$, 1.40 (H-16, H-16').

Using the HMBC data (Fig. 2), we were able to assemble different fragments. For example, rings A and B were linked together through the correlation pattern of C-5 at $\delta = 44.9$ with the methyl protons at $\delta = 0.88$ (CH_3-23) and 0.86 (CH_3-22). The connection of rings B and C and two other linkages (rings C and D) and the last pair of rings, D and E, were assembled together using the aforementioned TOCSY correlations to construct the respective backbone moieties.

Adipedatol (2): Since the Adipedatol (**2**) spectrum showed so many overlapped proton signals, first, using the chemical shift and the multiplicity, four methyl singlets (at 0.80, 0.83, 0.78 and 1.32 and one signal at 0.98 for two equivalent methyls) were identified step by step (Table 2), the lower field AB pattern at 3.15 and 3.24 was assigned to the oxymethylene protons of C-19 and the broad quartet at $\delta = 2.30$ was assigned to the axial H-16 proton deshielded by the axial hydroxyl group attached to C-20. This hydroxyl displayed a broad signal at $\delta = 1.92$. In addition, the triplet signal at $\delta = 1.98$ was assigned to H-21 as it shows small coupling to H-17 and H-22. Next, the four relatively isolated proton signals were assigned to H-22 ax (1.88), H-16 eq (1.70) and to the broad doublet of H-5 (0.68). Finally, the signal at 0.73 (broad triplet) was assigned to the axial H-1. The remaining protons of **2** are subject to extreme overlapping, and are located between 1.00 and 1.60 ppm.

Table 2. Adipedatol **2**.

Posit.	DEPT	δ H1*	δ C*	COSY‡	TOCSY#	HMBCΔ	HSQC TOCSY†
1	CH_2	0.73 1.62	40.3	1.32^2, 1.62^1, 1.55^2, 0.73^1, 1.55^2, 1.32^2	1.62^1, 1.55^2, 1.32^3, 1.10^3, 1.32^2, 1.10^3, 0.73^1	0.80^{26}, 0.73^1, 1.62^1	1.10^3, 1.32^2, 0.73^1, 1.55^2, 1.62^1
2	CH_2	1.55 1.32	18.7	1.32^2, 1.10^3, 0.73^1, 1.10^3, 1.55^2, 1.62^1	1.32^2, 0.73^1, 1.10^3	1.55^2, 1.32^2	1.55^2, 1.32^1, 0.73^1, 1.62^1, 1.10^3, 1.32^3
3	CH_2	1.32 1.10	42.0	1.55^2, 1.62^1, 1.10^3 1.32^3, 1.55^2	1.62^1, 0.73^1, 1.55^2, 0.73^1, 1.32^2, 1.55^2	0.78^{24}, 0.83^{25}, 1.32^3, 1.10^3	0.73^1, 1.10^3, 1.32^3, 1.55^2, 1.62^1
4	C		33.2			0.78^{24}, 0.83^{25}	
5	CH	0.68	56.1	1.32^6, 1.50^6	1.25^7, 1.45^7, 1.32^6, 1.50^6	0.68^5, 0.83^{25}, 0.78^{24}	0.68^5, 1.45^7, 1.32^6, 1.25^7
6	CH_2	1.50 1.32	18.6	1.32^6, 1.45^7, 1.25^7, 1.50^6, 1.45^7, 1.25^7	0.68^5, 1.45^7, 1.25^7	1.50^6, 1.32^6	1.50^6, 1.32^6, 0.68^5, 1.45^7, 1.25^7
7	CH_2	1.45 1.25	33.5	1.50^6, 1.32^6, 1.25^7, 1.45^7, 1.50^6, 1.32^6	1.32^6, 1.25^7, 0.68^5, 1.45^7	0.95^{27}, 1.45^7, 1.25^7	0.68^5, 1.45^7, 1.25^7
8	C		41.9			0.95^{27}	

Table 2. (continuation)

9	CH	1.25	50.4	1.45[11]	1.30[11], 1.45[11], 1.50[12]	0.80[26], 0.95[27], 1.25[9]	1.50[11], 1.49[13], 1.25[9]
10	C		37.4			0.80[26]	
11	CH_2	1.30 1.45	23.5	1.45[11], 1.50[12], 1.30[11], 1.25[12]		1.45[11], 1.30[11]	1.50[13], 1.45[11], 1.30[11], 1.25[9]
12	CH_2	1.50 1.25	20.9	1.25[12], 1.30[11]		1.50[12], 1.25[12]	1.50[12], 1.49[13], 1.30[11], 1.25[9]
13	CH	1.49	47.7		1.25[12]	0.95[28], 1.50[12]	1.49[13], 1.50[12], 1.25[12], 1.30[11], 1.45[11]
14	C		42.0			0.95[28]	
15	CH_2	1.28 1.22	32.5		2.30[16], 1.20[17]	1.28[15], 0.95[28]	2.30[16], 1.98[21], 1.70[16], 1.20[17]
16	CH_2	1.70 2.30	22.5	1.20[17], 2.30[16], 1.28[15]	1.98[21], 2.30[16], 1.20[17], 1.98[21], 1.70[16], 1.28[15]	1.70[16], 2.30[16]	2.30[16], 1.98[21], 1.70[16], 1.28[15], 1.20[17]
17	CH	1.20	49.0	1.70[16], 1.98[21]		1.20[17]	1.98[21], 1.70[16], 1.28[15], 1.20[17], 2.30[16]
18	C		42.6				
19	CH_2	3.15 4.24	65.2				
20	C		99.4			3.15[19], 4.24[19]	
21	CH	1.98	46.2	1.58[23], 1.18[22], 1.55[23]	1.88[22], 1.18[22], 1.55[23], 1.58[23]		1.98[21], 1.88[22], 1.58[23], 1.18[22]
22	CH_2	1.88 1.18	35.2	1.58[23], 1.18[22], 1.55[23], 1.88[22]	1.98[21], 1.55[23], 1.18[22]	1.88[22], 1.18[22]	1.98[21], 1.88[22], 1.55[23], 1.18[22]
23	CH_2	1.58 1.55	27.0	1.58[23], 1.18[22], 1.88[22], 1.18[22]	1.55[23], 1.98[21], 1.88[22], 1.98[21]	1.58[23], 1.55[23]	1.98[21], 1.88[22], 1.55[23], 1.18[22]
24	CH_3	0.78	21.5	1.10[3], 0.83[25]		0.78[24], 0.83[25]	
25	CH_3	0.83	33.4	0.78[24]	0.78[24]	0.83[25], 0.78[24]	
26	CH_3	0.80	15.8	0.73[1]		0.80[26]	
27	CH_3	0.95	17.3	1.45[7]			
28	CH_3	0.95	16.6	1.30[15]			
29	CH_3	1.32	29.0			1.32[29]	

* $^1H/^{13}C$ 600/150 MHz in $CDCl_3$ solution. Chemical shifts confirmed by HSQC experiments; ‡ ^1H-^1H correlation between proton on *n* position through 2σ and 3σ bonds. Superscript indicate proton assignment; #1 ^1H-^1H correlation between proton 2σ, 3σ and more bonds. Superscript indicate proton assignment; $^{\Delta}{}^2J_{CH}$, $^3J_{CH}$; Superscript indicate carbon on *n* position correlated with proton through 2σ and 3σ bonds; † C-H correlation *n* σ bonds. Superscript indicate proton correlation with carbon on *n* position.

TOCSY experiments were used to complete the proton signal assignment (Fig. 4) starting from 2.30, 1.98, 0.68 and 0.73 ppm. As is shown in Fig. 4, the diagonal peak on δ = 2.30 (H-16 ax) correlates with four different protons at δ = 1.98 (H-21), 1.70 (H-16), 1.28 and 1.22 (H-15 and H-15'). Consequently, the diagonal peak at δ = 1.98 (H-21) displayed correlation *via* the cross peaks at δ = 1.88 (H-22), 1.58 and 1.55 (H-23 and H-23') and with H-22' at δ = 1.18.

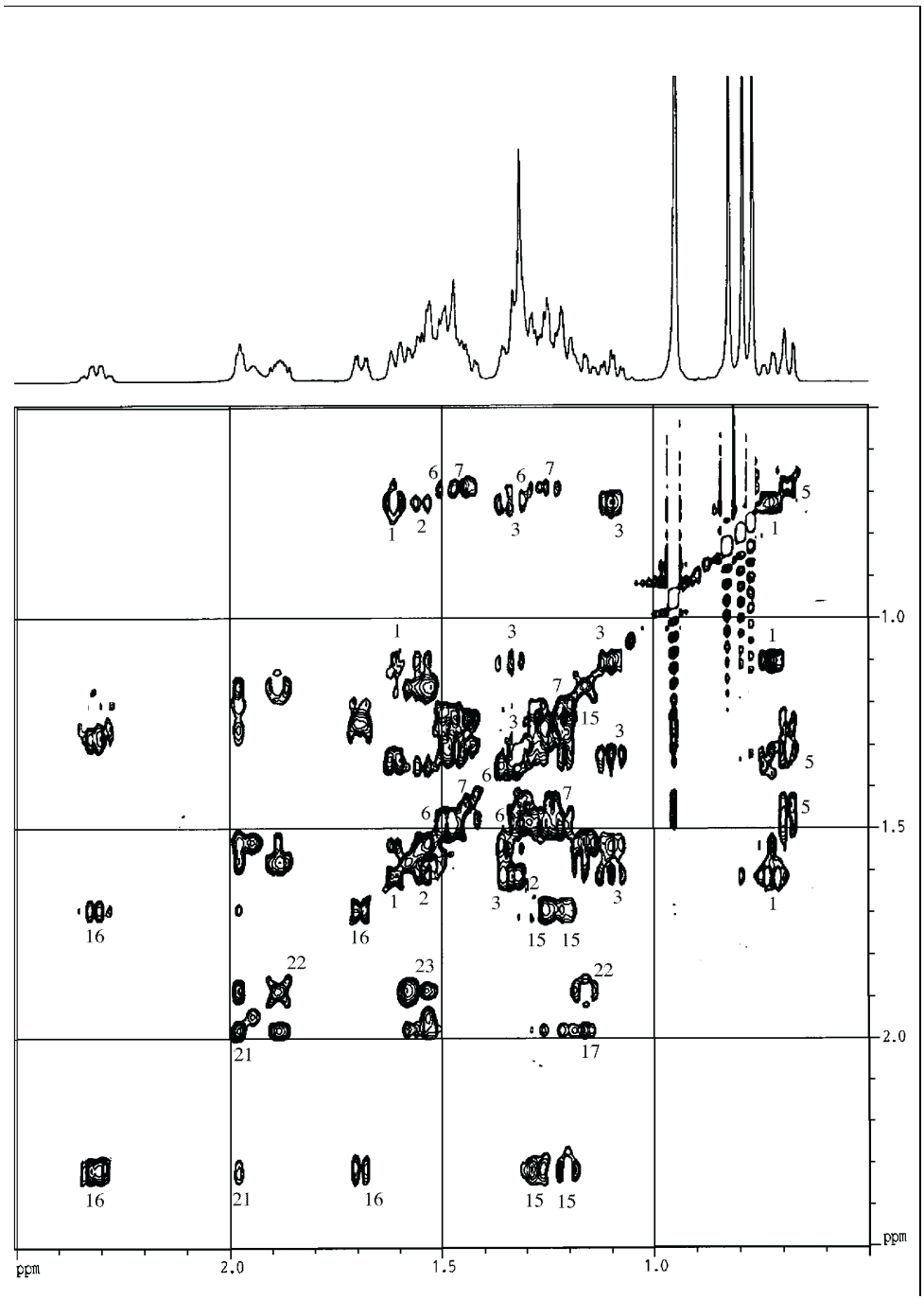

Figure 4. TOCSY spectrum of Adipedatol **2** recorded in $CDCl_3$ solution at ^{1}H RMN 600 MHz.

As in the previous case, this molecular segment C_{15}–C_{16}–C_{17}–C_{21}–C_{22}–C_{23} is also framed by the quaternary C-14 and C-18 carbons. The 3D $^{1}H/^{13}C$ NMR HSQC-TOCSY spectra (Fig. 5) clearly show the correlations used for the proton assignment of rings D and E. Using the diagonal peak of H-5 at $\delta = 0.68$, we were able to find cross peaks at δ = 1.50 (H-6), 1.32 (H-6'), 1.45 (H-7), 1.25 (H-7'). The molecular subunit C_5–C_6–C_7 is broken by the quaternary carbons C-4, C-10 and C-8.

The ring A protons form a fragment C_1–C_2–C_3 boarded by the quaternary carbons C-4 and C-10. The key element for the proton assignment here was the H-1 signal at δ = 0.73. Its diagonal peak at 0.73 ppm showed proton-proton connectivities with H-1' (δ = 1.62), H-2 (δ = 1.55), H-3 (δ = 1.32) and H-3' (δ = 1.10). The proton assignment for the rings A and B, as well as those of the rings D and E, was then confirmed by the use of the HSQC-TOCSY experiment (Fig. 5).

In the ^{13}C noise-decoupled NMR spectrum of **2** the signals with lowest chemical shift were assigned, according to Wehrli [16], to methylene C-1 at 40.3 and C-3 at 42.0. Both carbons assigned in this manner matched the proton chemical shifts for H-1, H-1', H-3 and H-3', as observed in HSQC-DEPT experiment (Fig. 6).

Ring C shows a fragment C_9–C_{11}–C_{12}–C_{13} bridged to the rest of the molecule by four quaternary carbons C-8, C-10, C-14 and C-18. Because of the small difference in chemical shifts between protons attached at C-9, C-11, C-12 and C-13, we were unable to directly perform the proton assignment through a TOCSY experiment. Nevertheless, by using the HSQC, the methine C-9 was located at $\delta_C = 50.4$ ($\delta_H = 1.25$); the CH_2-11 at $\delta_C = 23.5$ ($\delta_H = 1.30$ and 1.45), CH_2-12 at $\delta_C = 20.9$ ($\delta_H = 1.50$ and 1.25) and finally CH-13 at δ_C = 47.7 (δ_H = 1.49). The remaining methylene and methyl carbons were then easily assigned using HSQC and the chemical data in Table 2.

The next step in the structural assignment was the interconnection of these fragments. In order to determine the connectivity of the molecular backbone, long range ($^{2}J_{CH}$, $^{3}J_{CH}$) coupling information obtained from 2D $^{1}H/^{13}C$ NMR experiment (HMBC) was combined to the results of 3D $^{1}H/^{13}C$ NMR HSQC-TOCSY experiments. As seen in the HMBC experiment (Fig. 7), five methyls C-24, C-25, C-26, C-27, C-28, with three hydrogens each, fulfill all the necessary prerequisites for a diagnostically selective tool in the analysis of the molecule. For instance, the C-5 methine (δ_C = 56.1) displays 3σ bond correlations with CH_3-24 (δ_H = 0.78) and CH_3-25 (δ_H = 0.83) protons as well as 1σ bond correlation with H-5. All remaining correlations are shown in Table 2.

In order to obtain still greater insight into the structure of **2**, 3D NMR $^{1}H/^{13}C$ HSQC-TOCSY experiments were performed after which it was possible to observe carbon-proton correlations for protonated carbons through 1σ, 2σ, 3σ, 4σ and 5σ bonds. The most relevant correlations thus deduced from Fig. 5 are shown in Table 3. At this point, it can already be unambiguously determined how the aforementioned molecular fragments are attached. The methylene at δ_C = 65.2 has a chemical shift suggesting that such a carbon is in the vicinity of an oxygen atom. The quaternary carbon at δ = 99.4 clearly shows that such a signal corresponds to the hemiketal moiety of the structure HO–*C*(CH_3)–OCH_2–.

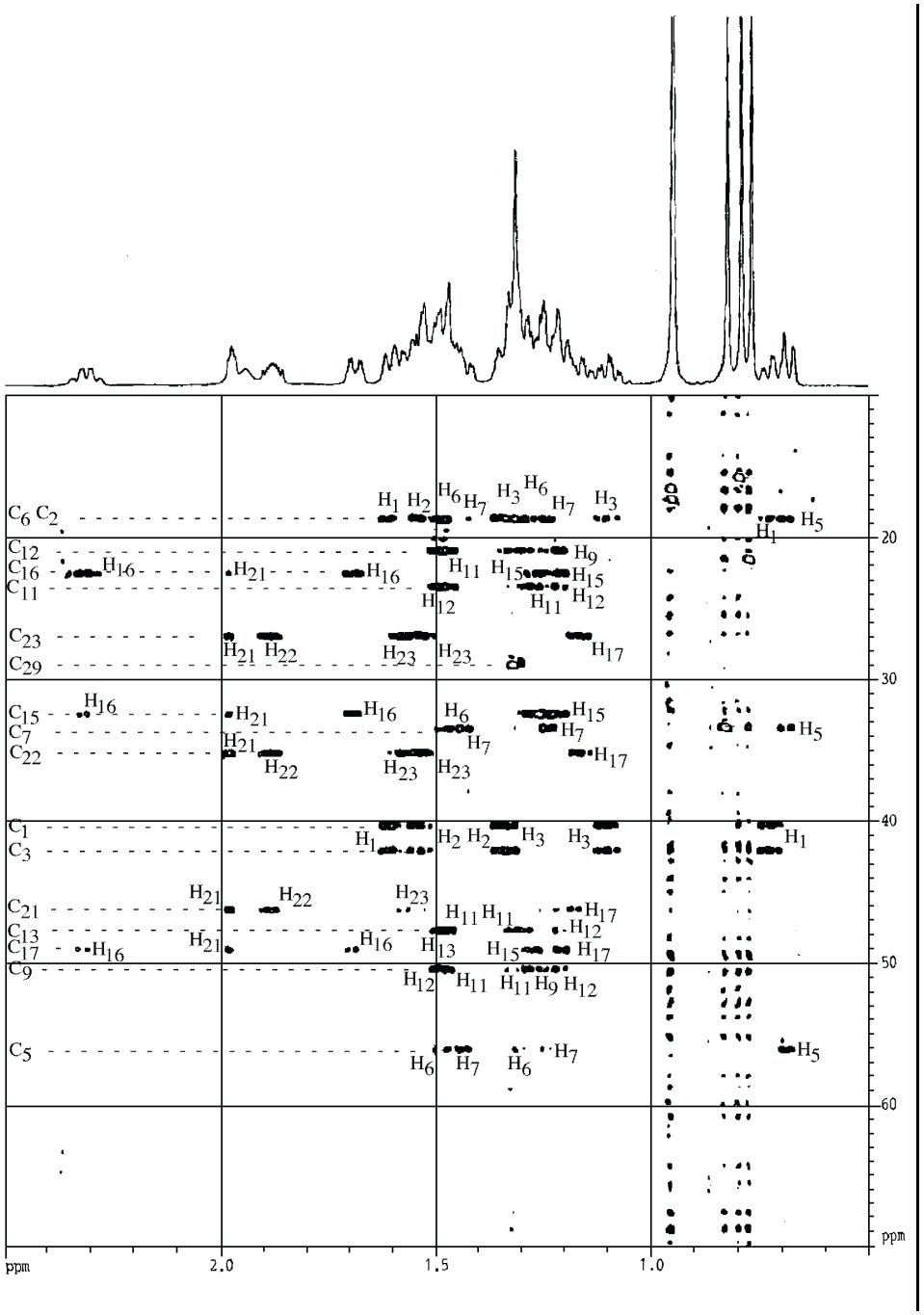

Figure 5. HSQC-TOCSY spectrum of Adipedatol **2** recorded in $CDCl_3$ solution at $^{1}H/^{13}C$ 600/150 MHz.

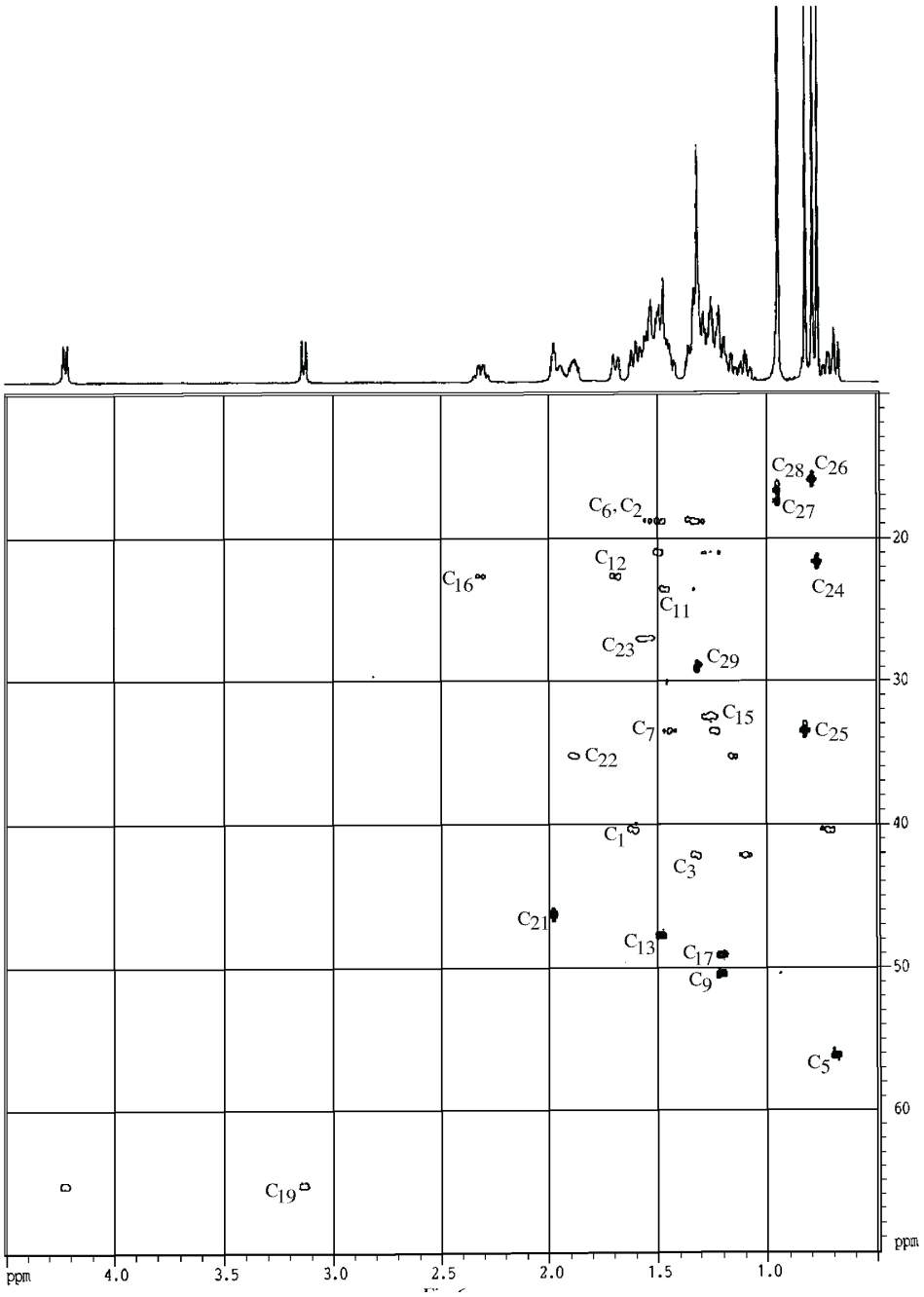

Figure 6. HSQC-DEPT spectrum of Adipedatol **2** recorded in $CDCl_3$ solution at $^{1}H/^{13}C$ 600/150 MHz.

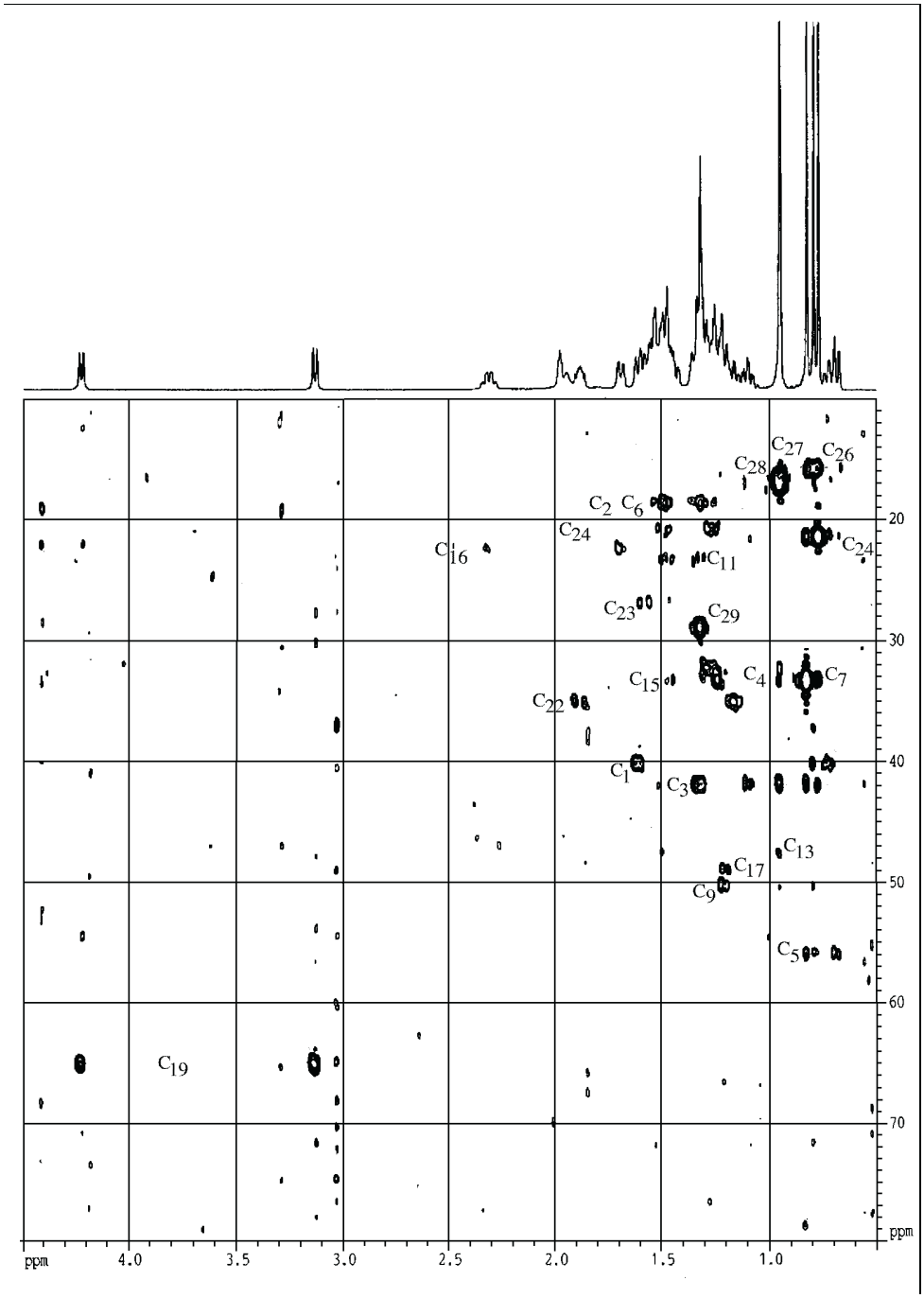

Figure 7. HMBC spectrum of Adipedatol **2** recorded in $CDCl_3$ solution at $^{1}H/^{13}C$ 600/150 MHz.

Table 3. Partial correlation scheme for **2**.

C#	δ_C (ppm)	Correlation with protons at
5	56.1	H-5, H-6, H-6', H-7, H-7'
9	50.4	H-12, H-11, H-11', H-12', H-9, H-13
17	49.0	H-16, H-21, H-16', H-15, H-17
13	47.7	H-11, H-11', H-12
21	46.2	H-21, H-22, H-23, H-17
3	42.0	H-1, H-2, H-3, H-3', H-1'
1	40.3	H-1, H-2, H-2', H-3, H-3', H-1'
2	18.7	H-1, H-2, H-3, H-3'
6	18.7	H-6, H-6', H-7, H-5
16	22.5	H-16, H-16', H-21, H-15, H-15'
23	27.0	H-21, H-22, H-23, H-23', H-17
15	32.5	H-16, H-21, H-16', H-15, H-15'
7	33.5	H-5, H-7, H-7', H-6
22	35.2	H-22, H-21, H-23, H-23', H-17

Since, even with the noise-decoupled ^{13}C-NMR spectrum, we were only able to observe five out of six quaternary carbons, and since the usual 2D NMR H/C techniques involve only protonated carbons, we have recorded an APT spectrum using a pulse delay of 4 msec. This C-spectrum displayed only the quaternary carbons and consequently enabled us to find the missed quaternary carbon covered by the methylene signal of C-3 at $\delta = 42.0$. The result of this experiment enabled us to detect two quaternary carbons at $\delta = 42.0$ and 41.9 assigned to C-14 and C-8, respectively.

These structures, as established by 2D and 3D NMR experiments, can only be challenged using X-ray crystallography techniques, undertaken after single-crystals of good quality were obtained. The molecular structures of the two compounds are represented in Figs. 8 and 9. Compound **2** crystallizes with three crystallographically independent, but nearly identical, molecules (denoted A, B and C), which are linked by intermolecular hydrogen bonds. The hydroxy group of molecule A is bound to that

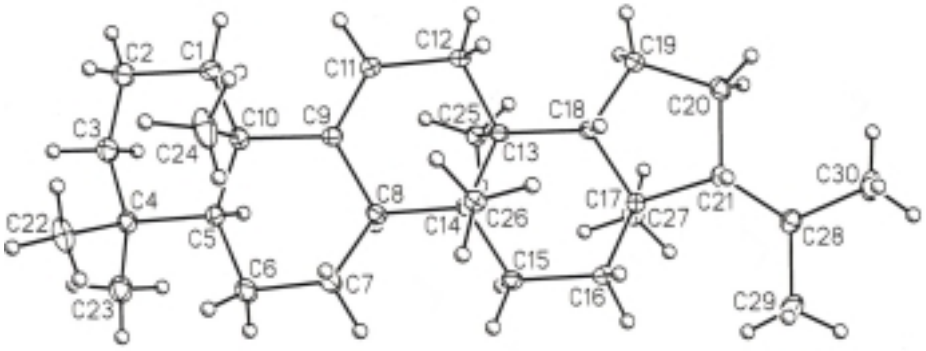

Figure 8. View of the molecular structure of Davallene. Ellipsoids are drawn at the 40% probability level. Hydrogen atoms are represented as small spheres of arbitrary radii.

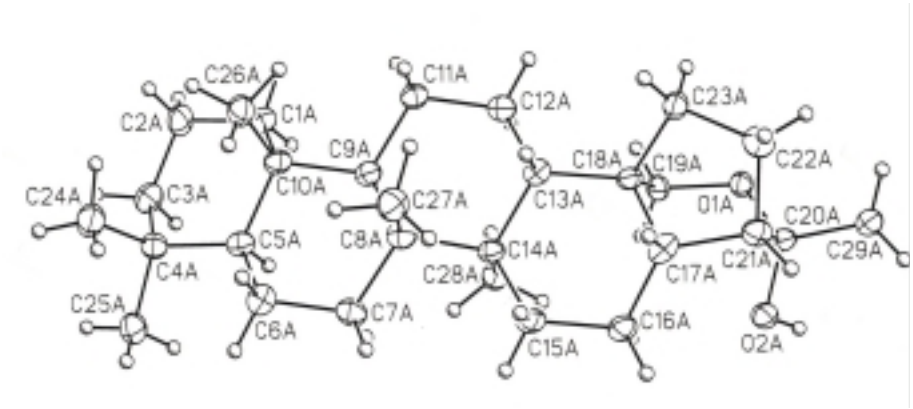

Figure 9. View of the molecular structure of Adipedatol. Ellipsoids are drawn at the 40% probability level. Hydrogen atoms are represented as small spheres of arbitrary radii.

of a neighbouring C molecule, with an O···O distance of 2.847(6) Å, the hydroxy group of molecule B is bound to the ether oxygen atom of a neighbouring B molecule [O···O distance 2.829(6) Å] and the hydroxy group of molecule C, apart from being a hydrogen bond acceptor from the hydroxy group of A, acts as a hydrogen bond donor towards the ether oxygen atom of another neighbouring A molecule [O···O distance of 2.835(5) Å].

CONCLUSIONS

The more complex the molecule and higher the number of spins, the sooner we reach a point at which spectral evaluation becomes difficult. This is thus expected for isomeric molecules containing only carbon and hydrogen (such as Davallene) or carbon, hydrogen and few oxygens (Adipedatol), so that it is difficult to unambiguously deduce their molecular structure, in particular elements which can provide valuable information on the number of cyclic-units. At this point, in addition to the usual $^{1}H/^{13}C$ 1D NMR and many variants of 2D NMR (COSY, TOCSY, HSQC and HMBC), the new and powerful 3D HSQC-TOCSY offers today a valuable alternative in both the initial and final approaches to structural analysis using NMR.

At the present time, in order to obtain more structural insights into these molecules, higher NMR frequencies (500 MHz or higher) have been used, improving the quality of interpretation of NMR spectra. However, in several cases, such as both triterpenes **1** and **2** described in this paper, the identification of the structures by NMR alone remains difficult even with 2D and 3D methods. The true breakthrough in structural elucidation is achieved with help, and *via* constant interaction between NMR and mass spectroscopy and in particular X-ray diffraction. With such data available, one can faster and more easily identify the triterpenic structures.

Finally, because of their wide variety of traditional medical applications, and in particular because of their worldwide occurrence, both triterpenes were tested on reverse transcriptase of the human virus type 1 inhibition (HIV-1 RT). Unfortunately, neither **1** nor **2** was a potential HIV-1 reverse transcriptase inhibitor [18].

EXPERIMENTAL

NMR materials and methods: The samples were dissolved in $CDCl_3$ and all NMR experiments were recorded at 27°C on a Bruker spectrometer operating at 600.0 MHz for ^1H and 150.0 MHz for ^{13}C nuclei. Chemical shifts are quoted in the delta δ scale, relative to the $CDCl_3$ resonance fixed at 7.24 ppm for the proton and 77.0 ppm for the carbon. The multiplicity of carbon signals was established by using the DEPT experiment. COSY spectra were collected into 800×1024 data matrix with 32 scans per t1 value and TOCSY spectra were collected with a mixing time of 80 ms into 512×1024 data matrix with 16 scans per t1 value. HSQC experiments were recorded with a delay of 3.5 ms ($^1J_{CH}$ = 143 Hz) and HSQC-TOCSY experiments with a mixing time for proton-proton transfer of 80 ms (400×1024) with 32 scans per t1 value to identify the one bond carbon-proton and the network of proton-proton connectivities, respectively. The HMBC experiment (400×1024) was recorded with a delay of 50 ms with 64 scans per t1 value to identify long range proton-carbon connectivities. All data were processed with the UXNMR software for both dimensions before Fourier transform. For HSQC, HSQC-TOCSY and HMBC data, a zero filling and $\pi/2$ phase shifted sine bell window function were applied in F2 dimension and a linear prediction was applied to 1024 points in F1 dimension prior to processing. The assignment of ^1H and ^{13}C resonances was carried out from analysis of COSY, TOSY, DEPT, HSQC, HSQC-TOCSY and HMBC data.

Plant materials: *Adiantum capillus-veneris* was collected in "Cerro del Alquitran" located at Km 11 on the Highway Acapulco to Mexico City, State of Guerrero, Mexico.

Isolation of compounds: The fronds were dried at room temperature, pulverized and extracted with hexane. Adipedatol **2** precipitated spontaneously from the original crude extract and was recrystallized from hexane to give colorless crystals with mp 170–173°C (reported 185–188°C [4]). The original crude extract subsequently underwent precipitation affording Davallene **1**, which was recrystallized from methylene chloride-methanol (1:1) yielding colorless crystals with mp 165–168°C (reported 175–177°C [5]).

Screening of HIV-1 RT inhibitors: Inhibition of reverse transcriptase of human virus type 1 (HIV-1 RT) by **1** and **2** were tested using a kit from Lenti RT assay (Cavidi Tech, Uppsala, Sweden). As positive control, nevirapine, a non nucleoside HIV reverse transcriptase inhibitor, was used. This compound was extracted with methylene chloride from commercial pills and then identified by ^1H NMR.

At the concentration tested, neither of these two terpenes inhibited significantly the HIV-1 reverse transcriptase activity. Nevertheless, the compound nevirapine at the highest concentration of 250 μM, used as a control, inhibited by 74% the incorporation of Br-desoxyuridine to a poly A nucleotide template.

Crystal structure determination: Compound **1** was recrystallized from hot CH_3OH and **2** from hot $CHCl_3/CH_3CN$ (1:1), both compounds giving single crystals (extremely thin colourless platelets) suitable for X-ray crystallography. Data were collected at 100(2) K on a Nonius Kappa-CCD area detector diffractometer [19] using graphite monochromated Mo-Kα radiation (λ 0.71073 Å). The crystals were introduced in Lindemann glass capillaries with a protecting "Paratone" oil (Exxon Chemical Ltd.) coating. The lattice parameters were determined from ten frames (ϕ-scans, 2° steps) and later refined on all data. A 180° ϕ-range was scanned with 2° steps with a crystal-to-detector distance fixed to 28 mm during data collection. The data were processed and corrected for Lorentz-polarization effects with DENZO-SMN [20]. The structures were solved by direct methods with SHELXS-97 [21] and subsequent Fourier-difference synthesis, and refined by full-matrix least-squares on F^2 with SHELXL-97 [21]. In the absence of suitable scatterers, the absolute configuration could not be determined in either compound. The Friedel pairs have in consequence been merged and the absolute configuration has been taken as

deduced from other investigations. All non-hydrogen atoms were refined with anisotropic displacement parameters. The hydrogen atoms bound to oxygen atoms in the three independent molecules of the structure of **2** were found on Fourier-difference maps. All other hydrogen atoms in both compounds were introduced at calculated positions. All these hydrogen atoms were treated as riding atoms, with an isotropic displacement parameter equal to 1.2 (OH, CH, CH_2) or 1.5 (CH_3) times that of the parent atom. The molecular plots were done with SHELXTL [22]. Crystal data and structure refinement details are given in Table 4. All calculations were performed on a Silicon Graphics R5000 workstation. CCDC reference numbers 208131 and 208132 contain the supplementary crystallographic data for this paper. These data can be obtained free of charge via www.ccdc.cam.ac.uk/conts/retrieving.html (or from the Cambridge Crystallographic Data Centre, 12, Union Road, Cambridge CB2 1EZ, UK; fax: +44 1223 336033; or deposit@ccdc.cam.ac.uk).

Table 4. Crystal data and structure refinement details.

	1	**2**
Chemical formula	$C_{30}H_{50}$	$C_{29}H_{48}O_2$
M/g mol^{-1}	410.70	428.67
Crystal system	orthorhombic	monoclinic
Space group	$P2_12_12_1$	$P2_1$
a/Å	7.6142(7)	18.3816(12)
b/Å	10.5875(9)	7.6447(5)
c/ Å	31.612(2)	26.9136(18)
β/°		102.325(4)
V/Å^3	2548.4(4)	3694.8(4)
Z	4	6
ρ_{calc}/g cm^{-3}	1.070	1.156
μ (MoKα)/mm^{-1}	0.059	0.070
Crystal size/mm	0.25 × 0.25 × 0.03	0.25 × 0.25 × 0.02
F(000)	920	1428
θ range/°	2.7–25.7	2.9–25.7
T/K	100(2)	100(2)
Number of data collected	17264	26531
Number of unique data	2711	7411
Number of "observed" data [$I > 2\sigma(I)$]	1960	4445
R_{int}	0.044	0.062
Number of parameters	279	856
R_1	0.054	0.068
wR_2	0.112	0.121
S	1.046	1.041
$\Delta\rho_{min}$/e Å^{-3}	–0.20	–0.26
$\Delta\rho_{max}$/e Å^{-3}	0.15	0.25

Acknowledgments

We thank some members of the Instituto de Quimica team, in particular Dr. M. I. Chavez for recording some of the NMR spectra, Drs. L. Velasco and D. Gaudin (CEA/Saclay, France) and J. Perez for mass spectra as well as Drs. M. Huertz and E. Velazquez for HIV testing.

REFERENCES

1. (*a*) Mickel J.T. and Beitel J.M., *Pteridophites. Flora de Oaxaca*, México. Mem. New York Bot. Garden, 1988, **46**, 1–568; (*b*) Moran R.C. and Riba R., *Psilotaceae a Salviniaceae*. *Flora Mesoamericana*. G. Davidse, M. Souza and S. Knapp, (Eds). Universidad Nacional Autonoma de México, **1**, 470 (1995).
2. Nakane T., Maeda Y., Ebihara H., Arai Y., Masuda K., Takano A., Ageta H., Shiojima K., Cai S.Q. and Abdel-Halim O.B., *Chem. Pharm. Bull.*, **50**, 1273 (2002).
3. Nakane T., Arai Y., Masuda K., Ishizaki Y., Ageta H. and Shiojima K., *Chem. Pharm. Bull*., **47**, 543 (1999); **42**, 39 (1994); **41**, 268 (1993).
4. Ageta H. and Iwata K., *Tetrahedron Lett*., **48**, 6069 (1966).
5. Ageta H. and Shiojima K., *J. Chem. Soc., Chem. Commun*., 1372 (1968).
6. Argueta-Villamar A., Cano L.M. and Rodarte M.E. (Eds). *Atlas de las Plantas de la Medicina Tradicional Mexicana*. Instituto Nacional Indigenista. México., **1**, 442 (1994).
7. Sengupta P., Dutt C.P., Sen M., Das K., Miyahara K. and Kawasaki T., *Indian J. Chem.*, **228**, 883 (1983).
8. (*a*) Derome A., in *Modern Techniques for Chemistry Research*, Pergamon Press. N.Y. 1987, p. 240; (*b*) Freeman R., *Spin Choreography. Basic Steps in High Resolution in NMR Spectrum.* Oxford, 1997.
9. Hull W.E., in *2D NMR Spectroscopy for Chemist and Biochemist*. Chapter 2, W.R. Croasmum, R.M.K. Carlson (Eds.), VCH Publishers, N.Y. 1987.
10. Martin G.E. and Sektzer A.S., *Two Dimensional NMR Methods for Establishing Molecular Connectivity*, VCH Publishers, N.Y. 1988, p. 219.
11. Bodenhausen G. and Reuben D.J., *Chem. Phys. Lett*., **69**, 185 (1980).
12. (*a*) Wider G. and Wuthrich K., *J. Magn. Reson*., **102**, 239 (1993); (*b*) Muller L., *J. Am. Chem. Soc*., **101**, 4481 (1979); (*c*) Marek R., Kralik L. and Skelenar V., *Tetrahedron Lett*., **38**, 665 (1997); (*d*) Bax A., Griffey R.H. and Hawkins B.L., *J. Magn. Reson*., **55**, 301 (1983); (*e*) Bax A., Ikura M., Kay L., Torchia D.A. and Tschudin R., *J. Magn. Reson*., **86**, 304 (1990).
13. (*a*) Bax A. and Summers M.F., *J. Am. Chem. Soc*., **108**, 2093 (1986); (*b*) Pearson G.A., *J. Magn. Reson*., **64**, 487 (1985).
14. (*a*) Cavanagh J., Fairbrother W., Palmer III A. and Skelton N., in *Protein NMR Spectroscopy. Principles and Practice*. Academic Press 1996, USA Chapter 4, p. 637; (*b*) Griesinger C., Sorensen O.W. and Ernst R.R., *J. Magn. Reson.*, **90**, 433 (1989).
15. Lerner L. and Bax A., *J. Magn. Reson.*, **69**, 375 (1986).
16. Wehrli F.W. and Nishida T., *The Use of Carbon-13 NMR Spectroscopy in Natural Products Chemistry. Progress in the Chemistry of Organic Natural Products*., 1979 **36**, 1–216. Springer-Verlag, N.Y.
17. More terpene structure assignments *via* high-resolution NMR: (*a*) Weis R. and Seebache W., *Magn. Res. Chem*., **40**, 455 (2002); (*b*) Belsner K., Büchele B., Werz U., Syrovets T. and Simmet T., *Magn. Res. Chem*., **41**, 115 (2003); (*c*) Bouget-Bonnet S., Rochd M., Mutzenhardt P. and Henry M., *Magn. Res. Chem*., **40**, 618 (2002); (*d*) Weis R. and Seebache W., *Magn. Res. Chem*., **40**, 455 (2002); (*e*) Reynolds W.F., McLean S., Burke S.J. and Jacobs H., *Magn. Res. Chem*., **39**, 757 (2001); (*f*) Soliman H.S.M., Simon A., Toth G. and Duddeck H., *Magn. Res. Chem.,* **39**, 567 (2001); (*g*) Salazar G.C.M., Silva G.D.F., Duarte L.P., Vieira Filho S.A. and Lula I.S., *Magn. Res. Chem*., **38**, 977 (2000); (*h*) Joshi B.S., Singh K.L. and Roy R., *Magn. Res. Chem*., **37**, 295 (1999); (*i*) Sahu N.P., Koike K., Jia Z., Mondal N.B., Achari B. and Nikaido T., *Magn. Res. Chem*.,, **37**, 152 (1999); (*j*) Elgamal M.H.A., Soliman H.S.M., Toth G., Halasz J. and Duddeck H., *Magn. Res. Chem*., **34**, 697 (1996); (*k*) Ascenso J.R. and Ferreira M.J.U., *Magn. Res. Chem*., **35**, 643 (1997); (*l*) Elgamal M.H.A., Soliman H.S.M., Elmunajjed D.T., Toth G., Simon A. and Duddeck H., *Magn. Res. Chem*., **35**, 637 (1997); (*m*) Toth G., Simon A., Elgamal M.H.A., Soliman H.S.M., Elmunajjed D.T. and Horvath G., *Magn. Res. Chem*., **36**, 376 (1998); (*n*) Elgamal M.H.A., Soliman H.S.M., Elmunajjed D.T., Toth G., Simon A. and Duddeck H., *Magn. Res. Chem*., **36**, 151 (1998).
18. Lenti Kit R.T. (Cavadi, Tech., Uppsala, Sweden) compared to nevirapine, a non-nucleoside HIV reverse transcriptase inhibitor.
19. Kappa-CCD software, Nonius BV, Delft, The Netherlands, 1998.
20. Otwinowski Z. and Minor W., *Methods Enzymol*., **276**, 307 (1997).
21. Sheldrick G.M., SHELXS-97 and SHELXL-97, University of Göttingen, Germany, 1997.
22. Sheldrick G.M., SHELXTL, Version 5.1, Bruker AXS Inc., Madison, WI, USA, 1999.